

Detecting pulsars in the Galactic centre

K. M. Rajwade^{1,2*}, D. R. Lorimer^{1,2,3} and L. D. Anderson^{1,2,3}

1. Department of Physics and Astronomy, West Virginia University, Morgantown, WV 26506, USA

2. Center for Gravitational Waves and Cosmology, West Virginia University, Chestnut Ridge Research Building, Morgantown, WV 26505, USA

3. Green Bank Observatory, Green Bank, WV 24944, USA

2 June 2022

ABSTRACT

Although high-sensitivity surveys have revealed a number of highly dispersed pulsars in the inner Galaxy, none have so far been found in the Galactic centre (GC) region, which we define to be within a projected distance of 1 pc from Sgr A*. This null result is surprising given that several independent lines of evidence predict a sizeable population of neutron stars in the region. Here, we present a detailed analysis of both the canonical and millisecond pulsar populations in the GC and consider free-free absorption and multi-path scattering to be the two main sources of flux mitigation. We demonstrate the sensitivity limits of previous surveys are not sufficient to detect GC pulsar population, and investigate the optimum observing frequency for future surveys. Depending on the degree of scattering and free-free absorption in the GC, current surveys constrain the size of the potentially observable population (i.e. those beaming towards us) to be up to 50 canonical pulsars and 1430 millisecond pulsars. We find that the optimum frequency for future surveys is in the range of 9–13 GHz. We also predict that future deeper surveys with the Square Kilometre array will probe a significant portion of the existing radio pulsar population in the GC.

Key words: Pulsars:general — Galaxy:centre — scattering — radiative transfer.

1 INTRODUCTION

Understanding the stellar populations in the Galactic centre (GC) region, and how they relate to the central super-massive black hole (Sgr A*), is a major goal of modern astrophysics. The central few parsecs of the Galaxy are known to consist of large molecular complexes and have high stellar densities compared to the rest of the Galactic disk (see, e.g., Schödel et al. 2007). Under these circumstances, many authors have already made the reasonable assumption that a large population of neutron stars exist in the GC (Morris & Serabyn 1996; Genzel et al. 2010).

Motivated by the promise of finding pulsars orbiting Sgr A*, there have been multiple surveys of the GC region (Johnston et al. 2006; Macquart et al. 2010; Deneva 2010; Bates et al. 2011). These surveys are typically conducted at frequencies higher than ~ 1 GHz to reduce the impact of interstellar scattering, which is known to cause potentially significant pulse broadening along lines of sight to pulsars in the inner Galaxy (Cordes & Lazio 1997). To date, no pulsars have been found in the GC region which we define in this paper to be within 1 pc of Sgr A* (i.e. an angular offset of $25''$ for $R_0 = 8.3$ kpc). The discovery of a magnetar (Eatough et al. 2013; Mori et al. 2013) has brought

the problem of pulsars in the GC to fore again. The discovery led Chennamangalam & Lorimer (2014) to conclude that there are very few pulsars in the GC. These results seem puzzling, given the high stellar density of the GC. Also, angular broadening measurements of SGR 1745–2900 have revealed that the scattering along this line of sight is less than expected. Bower et al. (2014) claim that the scattering screen along the line of sight lies ~ 6 kpc away from the GC in the Scutum arm. These findings suggest that previous surveys should have discovered more pulsars in the GC, which makes their dearth baffling.

The presence of hot, ionized gas in the central parsec of our Galaxy (Pedlar et al. 1989; Gillessen et al. 2012) raises the question of whether absorption can affect detection of radio pulsars. Recent studies have shown free-free thermal absorption to be the primary source of gigahertz peaked spectra, where the flux density spectrum shows a turnover at frequencies of ~ 1 GHz in some pulsars found in dense ionized environments (Lewandowski et al. 2015; Rajwade et al. 2016). The GC environment suggests that absorption by ionized gas could decrease the observed flux from neutron stars beaming towards us.

Such a dense and highly turbulent environment can also be responsible for large scattering, thereby, reducing incoming pulsar radio flux in our line of sight. The effects of the interstellar medium (ISM) in the GC on pulsar fluxes have

* kmrajwade@mix.wvu.edu

been studied previously. Cordes & Lazio (1997) modeled multi-path scattering in the GC in terms of a thin screen near the centre. As a result, the radio pulses observed can be substantially broadened at lower frequencies. Wharton et al. (2012) studied various flux mitigation effects due to the ISM that can alter the incoming pulsar flux and result in a non-detection. Recently, Macquart & Kanekar (2015) proposed that the neutron star population of the GC is dominated by millisecond pulsars (MSPs). They also claimed that more sensitive, high frequency surveys in the future would be able to detect MSPs in the GC. Though a MSP population has been predicted in the past, the results of Macquart & Kanekar (2015) are based on the luminosity distribution of known pulsar population sample, which has an inherent luminosity bias since we only detect the brightest pulsars.

In this paper, we try to answer questions regarding the GC pulsar population by modeling the GC environment and accounting for observational selection biases. We simulate a pulsar population in the GC environment and study the effect of the GC environment on pulsar fluxes. We find the optimum frequency for future surveys based on the results of the simulation. Section 2 describes the simulations with different models considered. In Section 3, we present the results of the analysis and their implications.

2 SIMULATIONS

To place constraints on the number of pulsars in the GC, we simulated synthetic populations of pulsars using the `PsrPopPy` package (Bates et al. 2014), a python module based on the `psrpop` code developed earlier for population synthesis of pulsars (Lorimer et al. 2006). The inferred parameters from the known pulsar population in the Galaxy are biased due to various selection effects (see, e.g., Faucher-Giguère & Kaspi 2006). These effects are accounted for by `PsrPopPy` (see Bates et al. 2014, for details). `PsrPopPy` generates synthetic pulsar populations based on a set of pulsar parameters. These are then searched for in a simulated pulsar survey based on past survey parameters to determine the subset of pulsars, that are theoretically detectable.

We considered populations of canonical pulsars (CPs) and millisecond pulsars (MSPs) in our analysis with `PsrPopPy` (Bates et al. 2014). For both cases, we simulated the populations using the luminosity scaling with period and period derivative. Following previous authors, we parameterize the luminosity L in terms of period P and period derivative \dot{P} as a power law:

$$L = \gamma P^\alpha \dot{P}^\beta, \quad (1)$$

where α , β and γ are model parameters. For simplicity, following Faucher-Giguère & Kaspi (2006), we take $\alpha = -1.5$ and $\beta = 0.5$ which physically links L to be proportional to the square root of the pulsar's spin-down luminosity. To ensure that the properties simulated sample are comparable to the observed sample, we modified the constant of proportionality in this expression, γ so that the luminosity of the simulated sample that is detected in a simulated Parkes survey matches the observed detected sample in the same survey. To achieve this, we simulated a population of CPs and MSPs for different γ s and ran a Kolmogorov-Smirnov (K-S) test on the luminosity distributions of the simulated

and the observed sample for both sub-populations. Since the K-S probability beyond ~ 0.1 implies that the model and observed distributions are statistically indistinguishable (see, e.g., Press et al. 2002), we obtain a range of γ values for which the luminosities are consistent as shown in Fig. 1. The best γ was chosen for the case where we obtained the maximum K-S probability for the two detected populations. The best simulated populations were used for further analysis. The parameters used for simulation of both populations are given in Table 1. We note in passing here that the optimal values of γ found here imply population-averaged values of 2.1 mJy kpc^2 and 0.1 mJy kpc^2 for CPs and MSPs respectively. Although our analysis does not make any distinction between solitary and binary MSPs which appear to have different luminosities (Bailes et al. 1997; Burgay et al. 2013), it does clearly show that MSPs are intrinsically fainter radio sources than CPs.

We show the luminosity distribution of the synthetic CP and MSP population along with sensitivities of past surveys in Fig. 2. The figure also shows future SKA-MID¹ and ngVLA (Carilli et al. 2015) surveys with assumed telescope parameters. The results of the past surveys along with the ngVLA and SKA-MID survey are shown in Table 2. From this it is evident that, even without considering any effects of the GC environment on the pulsar fluxes, the past surveys have only been able to probe at most 2% of the total pulsar population in the GC. We also report upper limits on the population based in different models of flux mitigation in the ISM in the Table. We discuss the results later in the paper.

We scaled the derived luminosities of the simulated population at 1.4 GHz to different frequencies given in Table 3 for both populations assuming a normal distribution of spectral indices (Bates et al. 2013). Then, the corresponding observed flux density

$$S = \frac{L_\nu}{D_{GC}^2}, \quad (2)$$

where L_ν is the luminosity at a frequency ν (see Chennamanigam & Lorimer 2014, for details) and D_{GC} is the distance to the GC which is assumed to be 8.3 kpc (Bower et al. 2014).

We obtained fluxes for different frequencies from luminosities obtained in the simulations using Eq. 2. Then, using the models discussed in the subsequent sections, we multiplied the fluxes by the appropriate factors to account for the reduction due to three scenarios: (i) Scattering, where the flux is reduced due to multi-path scattering between the source and the observer; (ii) Free Free absorption, where the radio flux from the pulsar is absorbed by the intervening medium; (iii) Both scattering and free-free absorption playing a role in flux mitigation. Under these circumstances, we aim to constrain the best possible scenario for detecting pulsars in the GC as a function of observing frequency and distance of the scattering screen from the GC. We describe the different models used in the next section.

¹ https://www.skatelescope.org/wp-content/uploads/2012/07/SKA-TEL-SKO-DD-001-1_BaselineDesign1.pdf

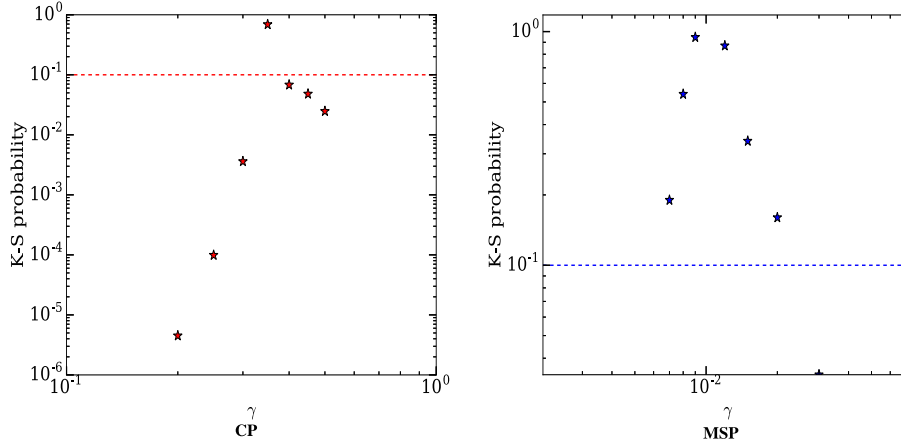


Figure 1. K-S probabilities of the luminosity distributions of observed and simulated samples versus γ . The horizontal line in each plot, shown for reference, represents a K-S probability of 0.1.

Parameter	CP	MSP
Radial distribution Model	Lorimer et al. (2006)	Lorimer et al. (2006)
Initial Galactic z -scale height	50 pc	50 pc
1-D velocity dispersion	265 km s ⁻¹	80 km s ⁻¹
Maximum initial age	1 Gyr	5 Gyr
Luminosity parameter α	-1.4	-1.4
Luminosity parameter β	0.5	0.5
Luminosity parameter γ	0.35	0.009
Spectral index Distribution	Gaussian	Gaussian
$\langle\alpha\rangle$	-1.4	-1.4
σ_α	0.9	0.9
Initial Spin period distribution	Gaussian	Log-Normal (Lorimer et al. 2015)
$\langle P \rangle$ (ms)	300	—
σ_P (ms)	150	—
$\langle \log_{10} P(\text{ms}) \rangle$	—	15
$std(\log_{10} P(\text{ms}))$	—	56
Pulsar spin-down model	Faucher-Giguère & Kaspi (2006)	Faucher-Giguère & Kaspi (2006)
Beam alignment model	orthogonal	orthogonal
Braking Index	3.0	3.0
Initial B-field distribution	Log-normal	Log-normal
$\langle \log_{10} B(\text{G}) \rangle$	12	8
$std(\log_{10} B(\text{G}))$	0.55	0.55
Scattering Model	Bhat et al. (2004)	Bhat et al. (2004)
Observed sample size	1065	39

Table 1. Table showing the different model parameters used in PsrPopPy for simulation of the two pulsar populations.

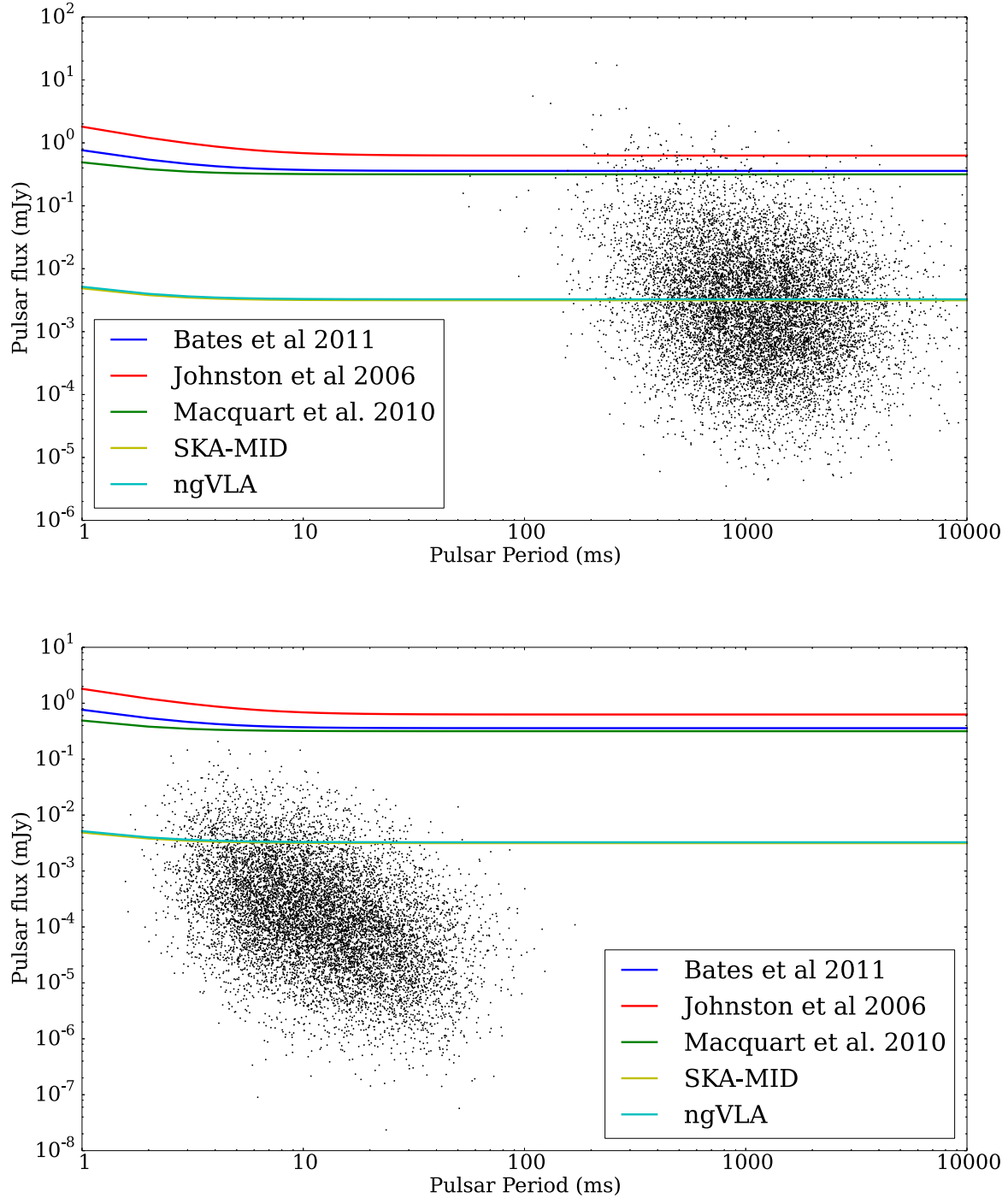


Figure 2. 1.4 GHz mean flux density versus period for a synthetic population of 10000 pulsars at the GC for the baseline model (BL). The top panel shows CPs while the bottom panel shows MSPs. Different lines indicate the survey sensitivities of past surveys apart from the SKA-MID survey. The parameters for SKA-MID survey are the expected parameters of the telescope. The sensitivities of each survey have been scaled to 1.4 GHz assuming a spectral index of -1.4 (Bates et al. 2013). The flux limit curves for each survey correspond to a DM of $1000 \text{ cm}^{-3} \text{ pc}$.

Model	A		B		Survey C		D		E	
BL	280/36	7/1429	212/47	7/1429	603/15	64/156	4623/2	1109/9	4652/2	1421/7
WS	280/36	7/1429	212/47	7/1429	603/15	64/156	4623/2	647/15	4652/2	1416/7
SS	212/47	0/-	201/50	0/-	603/15	11/909	2949/3	0/-	4650/2	13/769
FF	275/36	7/1429	210/48	7/1429	603/15	64/156	4600/2	1097/9	4647/2	1416/7
FF+WS	276/36	7/1429	210/48	7/1429	603/17	64/156	4593/2	638/16	4647/2	1412/7
FF+SS	208/48	0/-	199/50	0/-	603/17	11/909	2928/3	0/-	4640/2	13/769

Table 2. Table showing the number of pulsars that would have been detected in previous surveys from a sample 10,000 pulsars simulated at the GC for different models and the upper limit on the population for a null result in the survey. The surveys considered here are: (A) Bates et al. (2011); (B) Johnston et al. (2006); (C) Macquart et al. (2010); (D) SKA-MID survey; (E) ngVLA survey. The models listed are: (1) the baseline (BL) model with no scattering or free-free absorption; (2) weak scattering (WS); (3) strong scattering (SS); (4) free-free absorption (FF); (5) free-free and weak scattering (FF+WS); (6) free-free and strong scattering (FF+SS). Each pair of entries in the table gives the number of detections (n) out of the 10,000 as well as the simple upper limit ($10^4/n$) for CPs and MSPs. For example, in the baseline model for survey A, 280 CPs were detected implying an upper limit of 36 while 7 MSPs were detected implying an upper limit of 1429.

2.1 Model

In an attempt to make sense of the lack of pulsars in the GC found so far, we developed a model described below that takes account of multi-path scattering and free-free absorption effects on the pulsar signal. If S_0 is the intrinsic flux density of a pulsar at a frequency ν , then the measured flux density at the telescope

$$S_\nu = S_{0,\nu} \mathcal{S}(\nu) \mathcal{F}(\nu), \quad (3)$$

where $\mathcal{S}(\nu)$ and $\mathcal{F}(\nu)$ are the flux mitigation factors due to scattering and free free absorption respectively. These factors are discussed in turn in the sections below.

2.1.1 Free-Free absorption

Free-free absorption is known to bias flux density spectra of some pulsars (Lewandowski et al. 2015; Rajwade et al. 2016). This is manifested by a turnover in pulsar spectra at frequencies of ~ 1 GHz (Kijak et al. 2007, 2011) which is different from the turnover seen at lower frequencies due to synchrotron self absorption (Sieber 1973). This phenomenon is normally observed in pulsars that lie in dense environments like pulsar wind nebulae or supernova remnants. Since the GC consists of dense, ionized gas and cold molecular gas with thin ionization fronts, we assume free-free absorption plays a part in reducing the flux density of an expected pulsar population at the GC. If τ is the optical depth along a given line of sight then, as we showed in Rajwade et al. (2016), the observed flux

$$S_{\text{obs},\nu} = S_{\text{ref},\nu_{\text{ref}}} \left(\frac{\nu}{\nu_{\text{ref}}} \right)^\alpha \mathcal{F}(\nu), \quad (4)$$

where

$$\mathcal{F}(\nu) = \exp \left[-\tau_\nu \left(\frac{\nu}{\nu_{\text{ref}}} \right)^{-2.1} \right], \quad (5)$$

and $S_{\text{ref},\nu_{\text{ref}}}$ is the pulsar's observed flux density at a reference frequency ν_{ref} at which $\tau_\nu \ll 1$. For a Gaunt factor of

order unity², the optical depth

$$\tau_\nu = 0.082 \left(\frac{\nu}{\text{GHz}} \right)^{-2.1} \left(\frac{\text{EM}}{\text{cm}^{-6} \text{ pc}} \right) \left(\frac{T_e}{\text{K}} \right)^{-1.35}. \quad (6)$$

For this analysis, following Pedlar et al. (1989), we adopt an emission measure $\text{EM} = 5 \times 10^5 \text{ cm}^{-3} \text{ pc}$ and electron temperature $T_e = 5000 \text{ K}$ for the GC. Rajwade et al. (2016) shows that this effect is smaller at frequencies greater than ~ 1 GHz, which will be discussed later.

2.1.2 Scattering

Given a flux density spectrum that is modified by free-free absorption in the GC region, we also need to consider the impact of multi-path scattering. Observations of scatter-broadened pulse profiles, which are typically in the form of a one-sided exponential, have long been known to be powerful probes of the physical composition and structure of the ISM (for a review, see e.g., Bhat et al. 2004). Since the GC is a region with high stellar density and large amounts of molecular and ionized gas, a significant amount of scattering is expected for pulsars in this region. From (Cordes & Lazio 1997), for observations at some frequency ν of scattering due to a thin screen, the corresponding scattering timescale

$$t_{\text{sca}}(\Delta_{\text{GC}}) = 6.3 \text{ s} \left(\frac{D_{\text{GC}}}{8.5 \text{ kpc}} \right) \left(\frac{\theta_{\text{GC},1 \text{ GHz}}}{1.3''} \right)^2 \left(\frac{\nu}{\text{GHz}} \right)^{-4} \left(\frac{D_{\text{GC}}}{\Delta_{\text{GC}}} \right) \left(1 - \frac{\Delta_{\text{GC}}}{D_{\text{GC}}} \right). \quad (7)$$

In this expression, D_{GC} is the distance to the GC, Δ_{GC} is the distance of the scattering screen from the GC and θ_{GC} is the angular broadening of Sgr A* scaled to a frequency of 1 GHz. A pulse that is scatter broadened by a timescale t_{sca} will have its flux density altered. As shown by (Cordes & Lazio 1997), for a pulsar of period P , with intrinsic flux density S_ν at some frequency ν , the observed flux density

$$S_{\text{obs}} = S_\nu \exp \left[- \left(\frac{t_{\text{sca}} \pi}{2\sqrt{\ln 2} P} \right) \right]. \quad (8)$$

² This assumption is reasonable so long as $T_e > 20 \text{ K}$, which is the case in this work.

The position of the scattering screen towards the GC is still uncertain. For this analysis, we assume strong scattering scenario with the screen at ~ 100 pc (Cordes & Lazio 1997) and weak scattering with screen at ~ 6 kpc from the GC (Bower et al. 2014).

2.2 Probability of detection

Finally, we computed a probability of detecting a single pulsar (CP and MSP) at the GC as a function of frequency and screen distance for each of the three scenarios (scattering, free-free absorption and both effects) by considering surveys of the GC with the Green Bank Telescope (GBT). We selected the GBT because it is one of the largest fully steerable single dish telescope where one can observe the GC for a significant duration. We adopted the known parameters of Green Bank Telescope (GBT) receivers from the GBT observing guide³ to compute the flux limit at different frequencies for future GBT surveys (see Table 3). The sky contribution from the GC to the system temperature is significant and since the GC transits at an elevation of $\sim 21^\circ$, it was necessary to account for the changes in the system temperature, T_{sys} at lower elevations. To do this we assumed, the system temperature of each receiver,

$$T_{\text{sys}} = T_{\text{GC}} + T_{\text{atm}} + T_{\text{rec}}, \quad (9)$$

where, T_{GC} is the contribution of the GC, T_{atm} is the contribution due to the atmosphere and T_{rec} is the constant receiver temperature. T_{GC} is computed by taking the weighted average of $T_0(\nu)$ over the band of the receiver where $T_0(\nu) = 350 \left(\frac{\nu}{2.7\text{GHz}}\right)^{-2.7}$ (Reich et al. 1990). For T_{atm} , we computed empirical relations between T_{atm} and elevation for each receiver which made use of data from the GBT sensitivity calculator⁴. Then, we computed the weighted average of T_{atm} over all hour angles of the source by taking into account the dependence of elevation with hour angle. The final T_{sys} is calculated by plugging in values for T_{GC} , T_{atm} and T_{rec} in Eq. 9. The final values of flux sensitivities are given in Table 3. For multi-beam receivers, we assumed only a single beam. In these calculations, we are not assuming any coherent summing of multiple epochs. Using the fluxes computed in the simulation, we obtained flux histograms of the synthesized population at different GBT frequencies and counted up the number of the pulsars above the flux threshold of each survey. The required detection probability is simply the ratio of pulsars above each survey threshold to the total number of pulsars simulated.

In 2012, a new backend was developed for the GBT. The VEGAS (Versatile GBT Astronomical Spectrometer) is currently being used observations (Bussa & VEGAS Development Team 2012). The backend consists of 8 different spectrometer banks and has a maximum total instantaneous bandwidth of 1250 MHz for pulsar observations. VEGAS is expected to be the primary backend for pulsar astronomy and will replace the Green Bank Ultimate Pulsar Processing Instrument (GUPPI) (Ransom et al. 2009) in the process.

Hence, in our analysis, we assume VEGAS to be the primary backend for future GBT pulsar surveys. Under these assumptions, we computed probability of detection for two scenarios: (a) the backend would be able to accommodate the entire bandwidth of each receiver; (b) using VEGAS as the backend in which case the bandwidth is limited to 1250 MHz. The 2-D histograms for both the cases are shown in Fig. 3 and Fig. 4.

2.3 Results

Tables 2 and 3 clearly summarize our results from the analysis mentioned above. Table 2 suggests that there is a much smaller population of CPs in the GC based on the null result of previous surveys compared to MSPs. This result agrees with the inference in (Macquart & Kanekar 2015) and also would explain the GeV excess in the GC (Yuan & Zhang 2014). The predicted lack of CPs would suggest that star formation is suppressed at the GC and that the existence of MSPs could be explained through capture of MSPs from globular cluster (Hooper & Linden 2016).

Table 2 shows the upper limits on the populations based on previous and future surveys for various models. The results point out that the based on the null results from previous surveys, we can obtain an upper limit on the CP and MSP population in the GC and clearly the numbers suggest a MSP dominated pulsar population in the region and the results do not reject an existence of CP population in the GC. Our results predict ~ 50 CPs beaming towards us which is higher than the number of beaming CPs predicted by Chennamangalam & Lorimer (2014) by a factor of 2. Moreover, with the expected performance of SKA-MID and ngVLA, we would be able to probe a sizeable population of GC pulsars which would give us much better constraints. The constraints on the pulsar population are less stringent as we include models for flux mitigation as we would detect a lesser fraction of the existing population due to the effects of the ISM. Table 3 summarizes probabilities of finding one pulsar in a potential GBT survey. Results show that CPs have a better prospect of being detected than MSPs though the absolute probability is only as high as 0.1.

3 DISCUSSION

Although the probability of detecting a single pulsar is greater than zero for higher frequencies, where scattering and absorption effects are negligible, the value itself is small. This can be attributed to the distance of the GC where the fluxes of pulsars in the GC would be so small that even without assuming any attenuation of the flux, we have been able to probe only a small fraction of the population. Irrespective of the dominance of sub populations in the GC (CP or MSP), the faintness of these sources due to the distance of the GC makes it difficult to detect them. This is clearly indicated by Fig. 2 where the survey sensitivity limit only encloses 0 – 2% of the total simulated population of CPs. This shows that we need deeper searches of the GC in the future if the environment does not play a role in affecting pulsar fluxes.

Figs. 3 and 4 show the probability of detection for different frequencies and screen distances for MSPs and CPs. The

³ <https://science.nrao.edu/facilities/gbt/proposing/GBTpg.pdf>

⁴ https://dss.gb.nrao.edu/calculator-ui/war/Calculator_ui.html

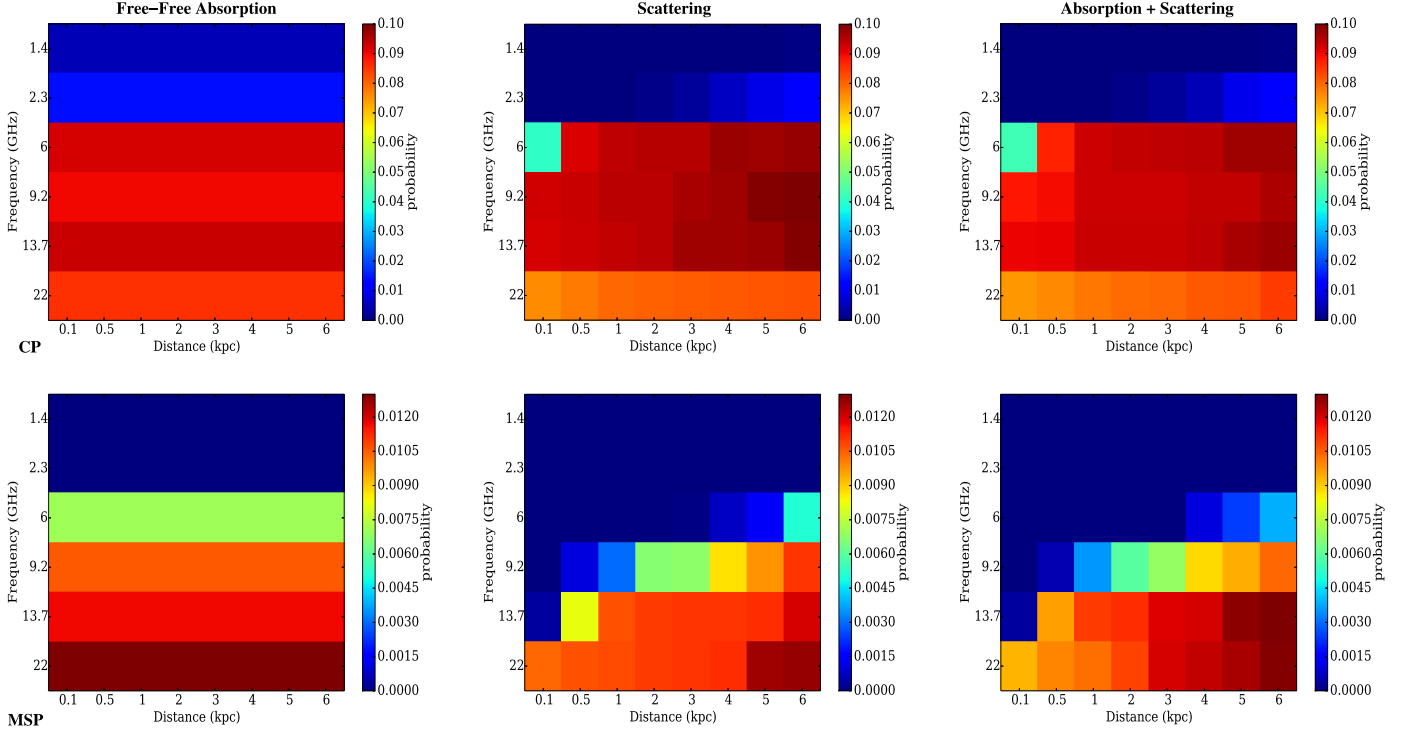


Figure 3. Probability of finding a pulsar in the GC as function of frequency and distance of the scattering screen from the GC in future GBT surveys assuming that the backend would be able to incorporate the whole bandwidth of each receiver. The columns from left to right are: free-free absorption, scattering, both scattering and absorption. The upper row is for CPs while the bottom one is for MSPs.

Receiver	Central Frequency	Bandwidth	Sensitivity Limit	VEGAS Limit	Detection probabilities expressed as percentages			
	(GHz)	(MHz)	μJy	μJy	Future backends		VEGAS	
					CP	MSP	CP	MSP
L-Band	1.4	650	590	590	≤ 0.5	0.0	≤ 0.5	0.0
S-Band	2.3	970	167	167	≤ 1.4	0.0	≤ 1.4	0.0
C-Band	6	3800	8.8	13.4	4–10	≤ 0.7	3–7	≤ 0.5
X-Band	9.2	2400	6.7	9.5	8–10	≤ 1	7–8	≤ 1.0
Ku-Band	13.7	3500	5.1	8.6	9–10	≤ 1.3	6–7.5	≤ 0.8
KFPA-Band	22	8000	5.4	13.7	7–8.5	0.9–1.3	4–5	0.4–0.6

Table 3. Table showing various parameters of the GBT receivers with corresponding survey limit for a future survey of the GC (see text for details). The details for receivers are given in <https://science.nrao.edu/facilities/gbt/facilities/gbt/proposing/GBTpg.pdf>.

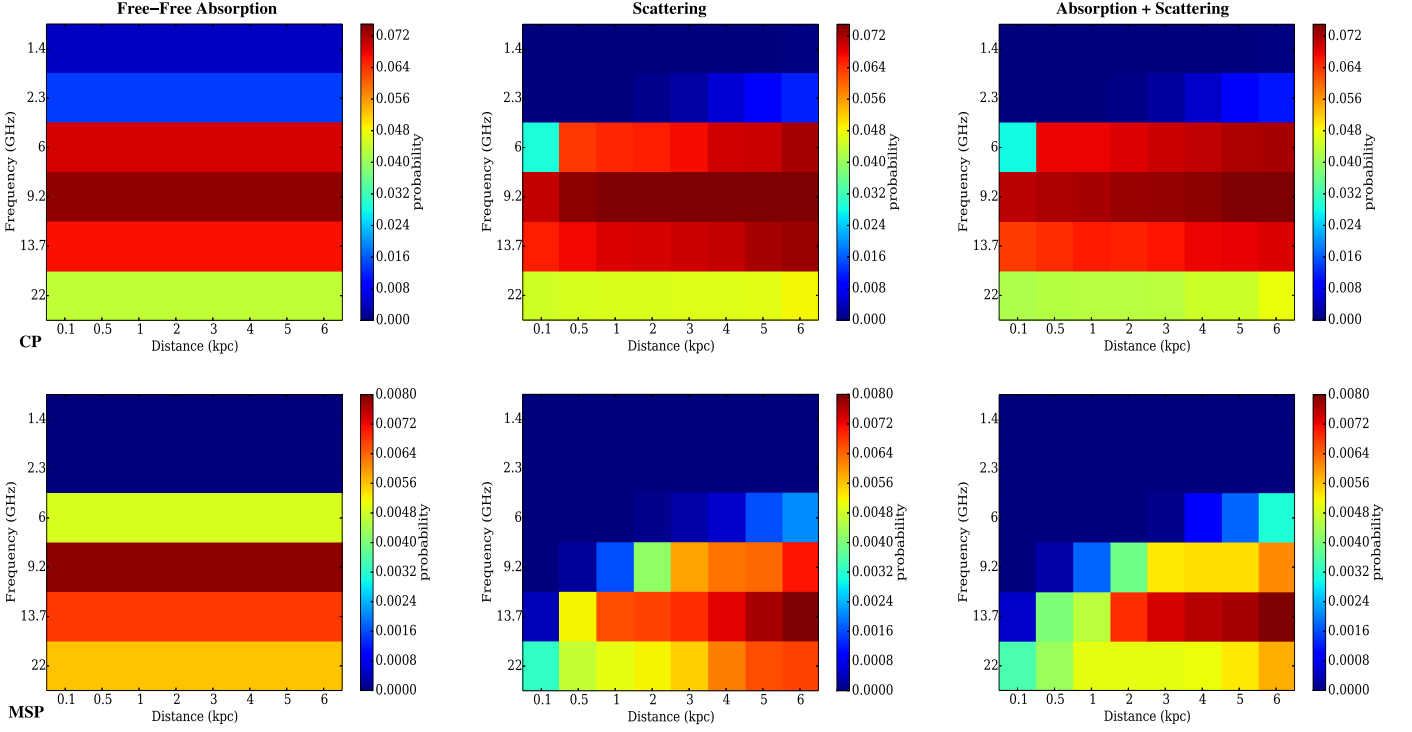


Figure 4. Probability of finding a pulsar in the GC as function of frequency and distance of the scattering screen from the GC. The probabilities have been computed for future GBT surveys and assuming VEGAS as the backend. The banding seen in the free free absorption case is due to the different bandwidths of receivers on the GBT.

figures show that free-free absorption has negligible effect on the flux mitigation beyond frequencies of 1 GHz due to negligible optical depths at higher frequencies. Hence, the probability of detection is solely dependent on the bandwidth of the telescope receivers. The banding structure evident in the figure is due to the fact that different GBT receivers have different bandwidths. On the other hand, scattering plays an important role in reducing flux from pulsars. Scattering transitions from strong scattering to weak scattering regime as the distance of the screen from the GC increases. Hence, one would expect to have maximum yield from the GC survey when the screen is far enough from the GC and the survey is at a high frequency. These aforementioned effects help us in constraining the optimum frequency for future GC surveys. Note that the optimum frequency largely depends on the bandwidth of the survey if it is backend limited. The 2-D histograms also suggest that the optimum frequency for future GBT surveys is as high as 9 GHz for CPs and 22 GHz for MSPs for strong and weak scattering cases if we assume the backends can cover the whole bandwidth of the receiver. On the other hand, if we consider VEGAS as the backend for future surveys, we obtain an optimum frequency of ~ 9 GHz for CPs for both, the strong and the weak scattering case. For MSPs, the optimum frequency is ~ 13 GHz for weak scattering case and > 22 GHz for the strong scattering case. These conclusions are in good agreement with the calculations in (Macquart & Kanekar 2015) however our results do not exclude the possibility of a CP population existing in the GC. In any case, we have to go to higher frequencies (> 9 GHz) to detect any pulsars in the GC in single observational tracks.

The results suggest that it would be more difficult to detect MSPs than CPs given the lower radio luminosities and the effect scattering has on their radio fluxes. We cannot favour any population at the moment because the analysis suggests that previous surveys have not been sensitive to any of the populations so far, even without factoring in the sources of flux mitigation. Our conclusions differ from Macquart & Kanekar (2015), which can be attributed to the fact that the population used by (Macquart & Kanekar 2015) is the actual pulsar population, which might have an inherent selection bias in the luminosity function of the source population as only the brightest pulsars have been detected by current radio telescopes. Hence, we sample only the tail of the underlying luminosity distribution of pulsars, which can lead to different inferences about the source population. On the other hand, we have considered a synthetic population of pulsars in the GC, assuming an underlying luminosity function, which properly accounts for this selection bias.

Recent results are suggesting that scattering does not play an important role in the attenuation of fluxes towards the GC. This is an important result for future surveys of the GC. If the weak scattering scenario is true then Fig. 2 suggests that deeper searches of the GC without going to higher and higher frequencies would result in more detections of pulsars. Future telescopes like the SKA and next generation Very Large Array (ngVLA) (Hughes et al. 2015) will provide a great opportunity to search for radio pulsars in the GC. These surveys are expected to detect significant fraction of the pulsar population in the inner Galaxy. Future high frequency radio surveys with highly sensitive radio telescopes will help in resolving the pulsar problem in the GC.

4 CONCLUSIONS

In summary, from an analysis of the current observational constraints of the pulsar population in the GC, our main conclusions are as follows: (i) the null results from previous surveys are not surprising, given that current surveys have only probed $\sim 2\%$ of the total pulsar population; (ii) upper limits on the CP and MSP population for various models constrain the population of pulsars beaming towards us to be < 50 CPs and < 1430 MSPs (iii) we predict the existence of CPs, along with MSPs in the GC though their numbers are expected to much smaller; (iv) a future GC survey with the GBT would have greater prospects of detecting CPs compared to MSPs. We find that the optimum frequency of a GBT survey would be 9–13 GHz; (v) a future surveys with SKA-MID and ngVLA would probe a sizeable population of the pulsar population in the GC.

REFERENCES

- Bailes M., Johnston S., Bell J. F., Lorimer D. R., Stappers B. W., Manchester R. N., Lyne A. G., Nicastro L., Gaensler B. M., 1997, *ApJ*, 481, 386
- Bates S. D., Johnston S., Lorimer D. R., Kramer M., Possenti A., Burgay M., Stappers B., Keith M. J., Lyne A., Bailes M., McLaughlin M. A., O’Brien J. T., Hobbs G., 2011, *MNRAS*, 411, 1575
- Bates S. D., Lorimer D. R., Rane A., Swiggum J., 2014, *MNRAS*, 439, 2893
- Bates S. D., Lorimer D. R., Verbiest J. P. W., 2013, *MNRAS*, 431, 1352
- Bhat N. D. R., Cordes J. M., Camilo F., Nice D. J., Lorimer D. R., 2004, *ApJ*, 605, 759
- Bower G. C., Deller A., Demorest P., Brunthaler A., Eatough R., Falcke H., Kramer M., Lee K. J., Spitler L., 2014, *ApJL*, 780, L2
- Burgay M., Bailes M., Bates S. D., Bhat N. D. R., Burke-Spolaor S., Champion D. J., Coster P., D’Amico N., et al. 2013, *MNRAS*, 433, 259
- Bussa S., VEGAS Development Team 2012, in American Astronomical Society Meeting Abstracts #219 Vol. 219 of American Astronomical Society Meeting Abstracts, VEGAS: VErsatile GBT Astronomical Spectrometer. p. 446.10
- Carilli C. L., McKinnon M., Ott J., Beasley A., Isella A., Murphy E., Leroy A., Casey C., et al. 2015, *ArXiv e-prints* 1510.06438
- Chennamangalam J., Lorimer D. R., 2014, *MNRAS*, 440, L86
- Cordes J. M., Lazio T. J. W., 1997, *ApJ*, 475, 557
- Deneva I. S., 2010, PhD thesis, Cornell University
- Eatough R., Karuppusamy R., Kramer M., Klein B., Champion D., Kraus A., Keane E., Bassa C., Lyne A., Lazarus P., Verbiest J., Freire P., Brunthaler A., Falcke H., 2013, *The Astronomer’s Telegram*, 5040
- Faucher-Giguère C.-A., Kaspi V. M., 2006, *ApJ*, 643, 332
- Genzel R., Eisenhauer F., Gillessen S., 2010, *Reviews of Modern Physics*, 82, 3121
- Gillessen S., Genzel R., Fritz T. K., Quataert E., Alig C., Burkert A., Cuadra J., Eisenhauer F., Pfuhl O., Dodds-Eden K., Gammie C. F., Ott T., 2012, *Nature*, 481, 51
- Hooper D., Linden T., 2016, *JCAP*, 8, 018
- Hughes A. M., Beasley A., Carilli C., 2015, *IAU General Assembly*, 22, 2255106
- Johnston S., Kramer M., Lorimer D. R., Lyne A. G., McLaughlin M., Klein B., Manchester R. N., 2006, *MNRAS*, 373, L6
- Kijak J., Gupta Y., Krzeszowski K., 2007, *A&A*, 462, 699
- Kijak J., Lewandowski W., Maron O., Gupta Y., Jessner A., 2011, *A&A*, 531, A16
- Lewandowski W., Rożko K., Kijak J., Melikidze G. I., 2015, *ApJ*, 808, 18
- Lorimer D. R., Esposito P., Manchester R. N., Possenti A., Lyne A. G., McLaughlin M. A., Kramer M., Hobbs G., Stairs I. H., Burgay M., Eatough R. P., Keith M. J., Faulkner A. J., D’Amico N., Camilo F., Corongiu A., Crawford F., 2015, *MNRAS*, 450, 2185
- Lorimer D. R., Faulkner A. J., Lyne A. G., Manchester R. N., Kramer M., McLaughlin M. A., Hobbs G., Possenti A., Stairs I. H., Camilo F., Burgay M., D’Amico N., Corongiu A., Crawford F., 2006, *MNRAS*, 372, 777
- Macquart J.-P., Kanekar N., 2015, *ApJ*, 805, 172
- Macquart J.-P., Kanekar N., Frail D. A., Ransom S. M., 2010, *ApJ*, 715, 939
- Mori K., Gotthelf E. V., Zhang S., An H., Baganoff F. K., Barrière N. M., Beloborodov A. M., Boggs S. E., Christensen F. E. e. a., 2013, *ApJL*, 770, L23
- Morris M., Serabyn E., 1996, *ARAA*, 34, 645
- Pedlar A., Anantharamaiah K. R., Ekers R. D., Goss W. M., van Gorkom J. H., Schwarz U. J., Zhao J.-H., 1989, *ApJ*, 342, 769
- Press W. H., Teukolsky S. A., Vetterling W. T., Flannery B. P., 2002, *Numerical recipes in C++ : the art of scientific computing*. Cambridge University Press
- Rajwade K., Lorimer D. R., Anderson L. D., 2016, *MNRAS*, 455, 493
- Ransom S. M., Demorest P., Ford J., McCullough R., Ray J., DuPlain R., Brandt P., 2009, in American Astronomical Society Meeting Abstracts #214 Vol. 214 of American Astronomical Society Meeting Abstracts, GUPPI: Green Bank Ultimate Pulsar Processing Instrument. p. 605.08
- Reich W., Fuerst E., Reich P., Reif K., 1990, *A&AS*, 85, 633
- Schödel R., Eckart A., Alexander T., Merritt D., Genzel R., Sternberg A., Meyer L., Kul F., Moutaka J., Ott T., Straubmeier C., 2007, *A&A*, 469, 125
- Sieber W., 1973, *A&A*, 28, 237
- Wharton R. S., Chatterjee S., Cordes J. M., Deneva J. S., Lazio T. J. W., 2012, *ApJ*, 753, 108
- Yuan Q., Zhang B., 2014, *Journal of High Energy Astrophysics*, 3, 1